Table II. Rate Constants (M^{-1} s^{-1}) for the Reaction

$$An + HY \underset{k_D}{\overset{k_F}{\rightleftharpoons}} AnY + H$$

	TMDTA		DCTA (8, 14)		EDTA (4,5)	
metal	$10^{-7}k_F$	$10^{-4}k_D$	$10^{-8}k_F$	k_D	$10^{-10}k_F$	$10^{-2}k_D$
Am	5.5 (±0.9)	4.78 (±0.49)	1.2	4.4	0.59	1.39
Cm	8.8 (±1.2)	3.52 (±0.22)	2.4	2.8	1.0	1.10
Bk	8.8 (±1.6)	0.95 (±0.10)			1.2	0.57
Cf	1.3 (±1.0)	0.39 (±0.02)			0.85	0.25
Eu	3.2 (±0.4)	2.29 (±0.13)	0.34	3.2	0.32	2.28

It has been proposed that this nonlinear behavior for log k_F reflects that the hydrated radii of the actinide cations do not have a direct inverse relation with the crystal radii.[17]

From these data, we can see how the structure of the ligand affects the formation rate constant of amino polycarboxylate chelates. The EDTA complexes have the fastest formation rate; the slower rate for the formation of DCTA chelates may be attributed to the stereochemical rigidity imposed by the cyclohexyl ring, and that for the TMDTA chelates may be attributed to the formation of the less stable six-membered N-M-N ring (in agreement with the observations of Kustin and co-workers).[18,19]

The relative dissociation rates also reflect the effect of the difference in stability between the five-membered N-M-N chelate ring in the EDTA complexes and the six-membered ring in the TMDTA chelates. Similarly, the stereochemical rigidity of the DCTA chelates can be invoked to explain the much lower rate of dissociation of these complexes compared to that of the An(EDTA) complexes.

Summary

A solvent extraction method has been used to study the dissociation kinetics of trivalent actinide chelates whose rate is moderately fast ($t_{1/2} < 1$ min). The dissociation of An(TMDTA)$^-$ proceeds through a proton-catalyzed pathway in which the first step is postulated to be the protonation of a carboxylate group in a fast equilibrium. The slow step is assigned to the dissociation of the nitrogen atom from the metal ion coupled to the formation of a hydrogen bond with the protonated carboxylate. The subsequent dissociation of the metal ion and the protonated ligand is rapid.

The dissociation rate constants decrease with metal ionic radius, which we attribute to decreasing nitrogen-metal bond lability. The increased chain length between the nitrogens causes a much larger dissociation rate than in the EDTA system. In general, the rate of dissociation of various actinide amino polycarboxylates depends on the stereochemistry of the ligand and the relative basicities of the nitrogen atoms.

Acknowledgment. This research was supported by a contract at FSU with the USDOE, OBES, Division of Chemical Sciences.

(17) Jones, A. D.; Choppin, G. R. *Actinides Rev.* **1969**, *1*, 311.
(18) Kustin, K.; Pasternak, R. F.; Weinstock, E. M. *J. Am. Chem. Soc.* **1966**, *88*, 4610.
(19) Kowalak, A.; Kustin, K.; Pasternak, R. R.; Petrucci, S. *J. Am. Chem. Soc.* **1967**, *89*, 3216.

Contribution from the Faculty of Pharmaceutical Sciences, Nagoya City University, Mizuho-ku, Nagoya 467, Japan

Conformational Interconversion Rates of 1,2-Diamine Chelates: Determination by Paramagnetic NMR Spectra of Low-Spin Iron(III) Complexes

Yoshitaka Kuroda, Noriko Tanaka, Masafumi Goto,* and Tomoya Sakai

Received July 15, 1988

The activation parameters for the $\delta \rightleftarrows \lambda$ interconversion of the five-membered diamine chelate rings in $[Fe(CN)_4(1,2\text{-diamine})]^-$ have been determined from a line-shape analysis of the paramagnetic ^1H NMR spectra by taking advantage of the large differences in chemical shift: $\Delta H^\ddagger$ = 24.7 ± 4.5, 30.1 ± 3.9, 42.7 ± 2.0 kJ mol^{-1}; $\Delta S^\ddagger$ = 0.0 ± 27.0, −2.9 ± 19.1, −7.7 ± 8.4 J K^{-1} mol^{-1}; $\Delta G^\ddagger_{298}$ = 24.7 ± 3.6, 31.0 ± 1.8, 45.0 ± 0.5 kJ mol^{-1} for ethanediamine, (2*R*,3*S*)-butanediamine, and (1*R*,2*S*)-*cis*-cyclohexanediamine. The effects of the alkyl groups on the rate of the interconversion are discussed. Temperature dependences of the paramagnetic shifts and the half line widths of the chelate ring protons for (*R*)-1,2-propanediamine and *N*,*N*'-dimethylethanediamine were measured, treated empirically, and employed for the calculation of the rate.

Introduction

Five-membered chelate rings formed by coordination of bidentate ligands, e.g., 1,2-diamines, diarsenes, thioethers, etc. to transition-metal ions have puckered conformations with either the δ or λ gauche form.[1] At room temperature the conformations of the chelate rings interconvert between δ and λ.[2,3] The populations of the two conformers have been investigated for diamine complexes of Co^{III},[4-11] Cr^0,[9,10] Mo^0,[9] Ru^{II},[5,12] Rh^{III},[13] Pd^{II},[4,9,14] Pt^{II},[4,9,15-22] Pt^{IV},[5,18] Ni^{II},[23-30] etc. by NMR spectroscopy. However, few informations about the dynamics of the conformational in-

(1) Corey, J.; Bailar, J. C., Jr. *J. Am. Chem. Soc.* **1959**, *81*, 2620.
(2) Hawkins, C. J.; Palmer, J. A. *Coord. Chem. Rev.* **1982**, *44*, 1.
(3) Tapscott, R. E.; Mather, J. D.; Them, T. F. *Coord. Chem. Rev.* **1979**, *29*, 87.
(4) Yano, S.; Ito, H.; Koike, Y.; Fujita, J.; Saito, K. *Bull. Chem. Soc. Jpn.* **1969**, *42*, 3184.
(5) Beattie, J. K.; Novak, L. H. *J. Am. Chem. Soc.* **1971**, *93*, 620.
(6) Sudmeier, J. L.; Blackmer, G. L.; Bradley, C. H.; Anet, F. A. *J. Am. Chem. Soc.* **1972**, *94*, 757.
(7) Tiethof, J. A.; Cooke, D. W. *Inorg. Chem.* **1972**, *11*, 315.
(8) Bagger, S.; Bang, O.; Woldbye, F. *Acta Chem. Scand.* **1973**, *27*, 2663.
(9) Hawkins, C. J.; Peachey, R. M. *Aust. J. Chem.* **1976**, *29*, 33.
(10) Toftlund, H.; Laier, T. *Acta Chem. Scand.* **1977**, *A31*, 651.
(11) Hilleary, C. J.; Them, T. F.; Tapscott, R. E. *Inorg. Chem.* **1980**, *19*, 102.
(12) Beattie, J. K.; Elsbernd, H. *J. Am. Chem. Soc.* **1970**, *92*, 1946.
(13) Sudmeier, J. L.; Blackmer, G. L. *Inorg. Chem.* **1971**, *10*, 2010.
(14) Pitner, T. P.; Martin, R. B. *J. Am. Chem. Soc.* **1971**, *93*, 4400.
(15) Erickson, L. E.; McDonald, J. W.; Howie, J. K.; Clow, R. P. *J. Am. Chem. Soc.* **1968**, *90*, 6371.
(16) Haake, P.; Turley, P. C. *J. Am. Chem. Soc.* **1968**, *90*, 2293.
(17) Appleton, T. G.; Hall, J. R. *Inorg. Chem.* **1970**, *9*, 1807.
(18) Appleton, T. G.; Hall, J. R. *Inorg. Chem.* **1971**, *10*, 1717.
(19) Erickson, L. E.; Erickson, M. D.; Smith, B. L. *Inorg. Chem.* **1973**, *12*, 412.
(20) Bagger, S. *Acta Chem. Scand.* **1974**, *A28*, 467.
(21) Erickson, L. E.; Sarneski, J. E.; Reilley, C. N. *Inorg. Chem.* **1975**, *14*, 3007.
(22) Lind, T.; Toftlund, H. *Acta Chem. Scand.* **1982**, *A36*, 489.
(23) Ho, F. F.-L.; Reilley, C. N. *Anal. Chem.* **1969**, *41*, 1835.
(24) Ho, F. F.-L.; Reilley, C. N. *Anal. Chem.* **1970**, *42*, 600.
(25) Ho, F. F.-L.; Erickson, L. E.; Watkins, S. R.; Reilley, C. N. *Inorg. Chem.* **1970**, *9*, 1139.

0020-1669/89/1328-0997$01.50/0

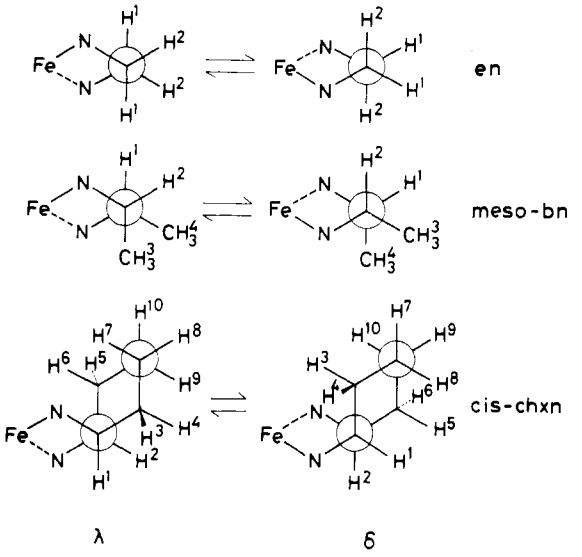

Figure 1. Conformational interconversion of five-membered chelate rings between δ and λ forms. Fe indicates $Fe(CN)_4$.

terconversion have been offered by these studies, although they have revealed the energy difference between the two conformers.

The determination of the rate and activation parameters for the $\delta \rightleftarrows \lambda$ interconversion is important in evaluation of the predominance of certain conformations of metal chelates and in understandings of dynamics played in transition-metal complexes. Unfortunately, such experimental data have been reported only for a few substituted diaminoethane chelates.[31-34]

The determination of the activation parameters for the unsubstituted systems, e.g., ethanediamine, is important as a reference for the investigation of the conformational dynamics. However, the $\delta \rightleftarrows \lambda$ interconversion in these systems is very fast on the NMR time scale. Many attempts have not succeeded in determining the energy barrier experimentally,[8,20,22,35] due to the small differences in chemical shift between the magnetically interconvertible two nuclei in the diamagnetic metal complexes used for the studies. This limit will be overcome by the use of paramagnetic metal complexes with large chemical shift differences, although the evaluation of the intrinsic values in a frozen conformation with respect to chemical shift and half line width of the chelate nuclei under rapid conformational interconversion will be complicated because these values are strongly dependent on temperature. Various Ni^{II}–diamine complexes[23-30] have been investigated to determine the activation parameters based on the large chemical shift difference between axial and equatorial protons on the five-membered chelate ring. However, the activation parameters measured are limited to those for $\Delta \rightleftarrows \Lambda$ isomerization of tris(diamine) complexes.[30]

Tetracyano(1,2-diamine)ferrate(III) complexes,[36-38] $[Fe(CN)_4(1,2\text{-diamine})]^-$, are favorable candidates for this purpose because of the following reasons: the chemical shift difference between the axial and equatorial ring protons in a frozen conformation is larger than ca. 30 ppm at room temperature,[39] and the mono(diamine)-chelate nature leaves no ambiguity from the interaction among chelate rings expected for bis or tris chelates.

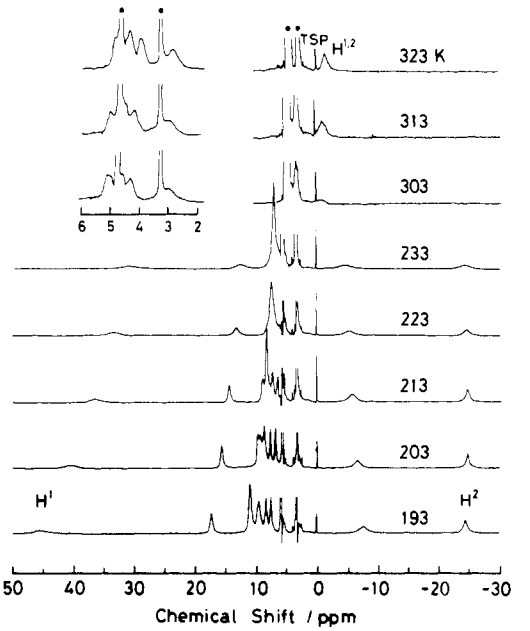

Figure 2. Temperature-dependent ^1H NMR spectra of $[Fe(CN)_4(cis\text{-chxn})]^-$ in CD_3OD–DCl. The numbering of the signals is related to the left conformer in Figure 1. The methylene signals of cyclohexane ring are shown in the inset. A dot (●) indicates a signal of the solvent.

We wish to report a determination of rates and activation parameters for the $\delta \rightleftarrows \lambda$ interconversion of three five-membered chelate rings, which were obtained for the low-spin Fe^{III} complexes of the general formula $[Fe(CN)_4(1,2\text{-diamine})]^-$ (1,2-diamine = ethanediamine (en), (2*R*,3*S*)-butanediamine (*meso*-bn), and (1*R*,2*S*)-*cis*-cyclohexanediamine (*cis*-chxn)) shown in Figure 1. The effects of the substituents on the activation parameters will also be discussed.

Experimental Section

Materials. Sodium tetracyano(1,2-diamine)ferrate(III), where 1,2-diamine = ethanediamine(en),[40] (2*R*,3*S*)-butanediamine (*meso*-bn),[41] (1*R*,2*S*)-*cis*-cyclohexanediamine (*cis*-chxn),[36] (*R*)-1,2-propanediamine (*R*-pn),[36] and *N*,*N*'-dimethylethanediamine (s-Me_2en)[40] were prepared as reported previously.

NMR Measurements. Variable-temperature ^1H NMR spectra of the Fe^{III} 1,2-diamine chelates in CD_3OD solution (containing 0.25% DCl) were recorded at 183–323 K with a JEOL FX-100 spectrometer. The concentrations of the chelates were ca. 0.05 mol dm^{-3} in order to prevent deposition of the chelates below 273 K. A total of 20–40 transients were collected for each sample at each temperature, yielding spectra with signal/noise ratios of ca. 20/1. ^1H NMR spectra of $[Fe(CN)_4(meso\text{-bn})]^-$ at 191 and 183 K were recorded with a JEOL GX-400 spectrometer. A total of 160 transients were collected. Probe temperatures were controlled with a JNM-VT-3C temperature control apparatus and determined from the chemical shift difference between the methyl and hydroxyl protons of methanol.[42] Sodium 3-(trimethylsilyl)propionate-2,2,3,3-d_4 (TSP) was used as an internal reference. The positive chemical shifts indicate downfield shifts from TSP.

Calculation of Half Line Width at Half-Height and Interconversion Rate Constant. The half line width at half-height and the interconversion rate were calculated by using the least-squares programs SALS[43] and MULTI[44] with a NEAC ACOS 850 computer of the computing center of this university.

(26) Evilia, R. F.; Young, D. C.; Reilley, C. N. *Inorg. Chem.* **1971**, *10*, 433.
(27) Cramer, R. E.; Harris, R. L. *Inorg. Chem.* **1973**, *12*, 2575; **1974**, *13*, 2208.
(28) Sarneski, J. E.; Reilley, C. N. *Inorg. Chem.* **1974**, *13*, 977.
(29) Cramer, R. E.; Huneke, J. T. *Inorg. Chem.* **1978**, *17*, 64.
(30) Hawkins, C. J.; Peachey, R. M. *Acta Chem. Scand.* **1978**, *A32*, 815.
(31) Caulton, K. G. *Inorg. Nucl. Chem. Lett.* **1973**, *9*, 533.
(32) Evans, D. F.; De Villardi, G. C. *J. Chem. Soc., Chem. Commun.* **1976**, 7.
(33) Hawkins, C. J.; Peachey, R. M.; Szoredi, C. L. *Aust. J. Chem.* **1978**, *31*, 973 and references therein.
(34) Desreux, J. F. *Inorg. Chem.* **1980**, *19*, 1319.
(35) Yano, S.; Ito, H.; Koike, Y.; Fujita, J.; Saito, K. *J. Chem. Soc. D* **1969**, 460.
(36) Goto, M.; Takeshita, M.; Sakai, T. *Bull. Chem. Soc. Jpn.* **1981**, *54*, 2491.
(37) Goto, M.; Takeshita, M.; Sakai, T. *Inorg. Chem.* **1978**, *17*, 314.
(38) Goedken, V. L. *J. Chem. Soc., Chem. Commun.* **1972**, 207.
(39) Kuroda, Y.; Goto, M.; Sakai, T. *Bull. Chem. Soc. Jpn.* **1987**, *60*, 3917.
(40) Goto, M.; Goedken, V. L. To be submitted for publication.
(41) Kuroda, Y.; Tanaka, N.; Goto, M.; Sakai, T. Submitted for publication.
(42) The probe temperature was calibrated by the use of the calibration chart supplied by JEOL.
(43) Nakagawa, T.; Koyanagi, Y. *Statistical Analysis with Least-Squares Fitting* (*SALS*); University of Tokyo: Tokyo, 1979.
(44) Yamaoka, K.; Tanigawara, Y.; Nakagawa, T.; Uno, T. *J. Pharmacobio-Dyn.* **1981**, *4*, 879.

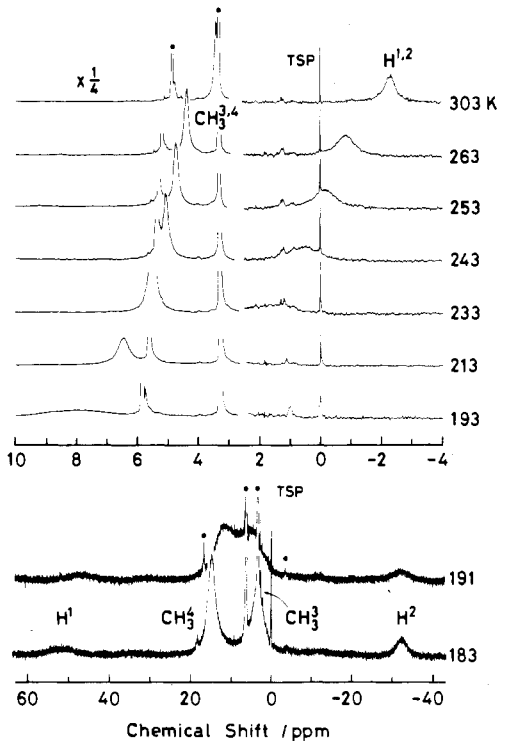

Figure 3. Temperature-dependent ^1H NMR spectra of $[Fe(CN)_4(meso\text{-bn})]^-$ in CD_3OD–DCl. The lower two spectra were taken on a GX-400 spectrometer and the others on a FX-100 spectrometer. The numbering of the signals is related to the left conformer in Figure 1. A dot (●) indicates a signal of the solvent and a spin noise. One of the two methyl signals overlaps with these solvent signals.

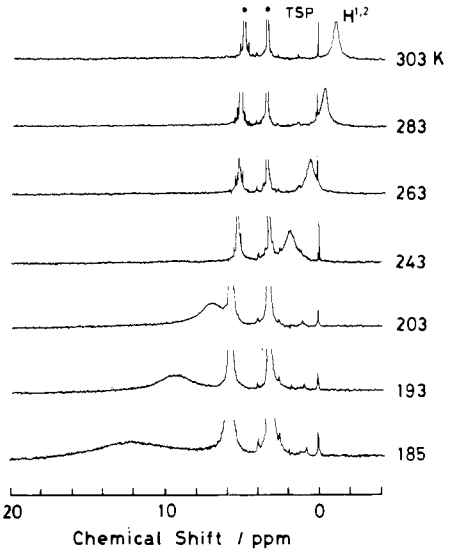

Figure 4. Temperature-dependent ^1H NMR spectra of $[Fe(CN)_4(en)]^-$ in CD_3OD–DCl. A dot (●) indicates a signal of the solvent.

Results

Variable-Temperature ^1H NMR Spectra. The variable-temperature 100-MHz ^1H NMR spectra of the low-spin Fe^{III} complexes $[Fe(CN)_4(1,2\text{-diamine})]^-$ (1,2-diamine = en, *meso*-bn, and *cis*-chxn), are presented in Figures 2–4. The temperature range was limited to 323–183 K by the boiling and freezing points of the solvent. The numbering for ^1H nuclei is denoted in Figure 1.

The *cis*-chxn chelate exhibited three peaks at 4.31, 3.94, and 2.87 ppm and one peak at −1.44 ppm at 323 K, as shown at the top of Figure 2. The former peaks overlap incidentally with signals of the solvents, and the enlarged spectra in this region are presented as insets in Figure 2. This chelate has 10 different protons as shown at the bottom of Figure 1, and if the conformations of the five-membered chelate and cyclohexane rings are fixed, 10 ^1H signals should be observed separately. The $\delta \rightleftarrows \lambda$ conformational interconversion of the chelate ring, as shown in Figure 1, changes the alkyl groups and ring protons (H^1 and H^2) from axial into equatorial and vice versa. If this interconversion is rapid enough, time-averaged signals between the δ and λ conformers are expected to be observed. Therefore, the spectra measured near room temperature indicate that this chelate ring undergoes $\delta \rightleftarrows \lambda$ conformational interconversion rapidly on the NMR time scale.

The peaks observed near room temperature were assigned by using rapid electron exchange between $[Fe^{II}(CN)_4(cis\text{-chxn})]^{2-}$ and $[Fe^{III}(CN)_4(cis\text{-chxn})]^-$.[41] The signals for the former complex have been already assigned.[41] The mixture of the two complexes showed ^1H signals at weighted averaged positions between the signals for the two components. The successive addition of the Fe^{III} complex to the Fe^{II} complex shifted each signal in proportion to the mole fraction of the Fe^{III} complex. This procedure correlates each signal of the Fe^{III} chelate to the corresponding signal of the Fe^{II} chelate. In this manner, the peak at ca. −1 ppm was assigned to the averaged signal of H^1 and H^2, and the peaks at 3–5 ppm were assigned to the other protons of the cyclohexane.[41]

The averaged signal of H^1 and H^2 shifted downfield accompanied by the line broadening with the decrease in temperature, and disappeared at 293 K. At 243 K, two separate signals appeared at both ends of the spectrum, and the chemical shift difference between them amounted to 69.8 ppm at 193 K. The downfield and upfield signals were assigned to H^1 and H^2, respectively, because (i) the chemical shift estimated by the extrapolation of chemical shift vs temperature plot for the averaged signal to 243 K was in agreement with the mean shift of the two peaks at both ends observed at 243 K, and (ii) Fe^{III} diamine complexes of this class exhibit upfield shifts for equatorial ring protons and most downfield shifts for axial protons, as reported previously.[41]

Another set of two peaks appeared at 243 K almost simultaneously with the appearance of H^1 and H^2 signals. These peaks were correlated to the averaged signal at 2.87 ppm observed at 323 K, and may probably be assigned to H^3 and H^6, which are nearest to the Fe ion second to H^1 and H^2 and are expected to have the second largest separation. The other averaged signals of the cyclohexane ring shifted downfield with the decrease in temperature, but began to separate at 213 K. At 193 K, eight peaks were observed at 45.45, 17.33, 10.88, 9.46, 8.33, 7.51, −7.52, and −24.36 ppm with an area ratio of 1:1:2:2:1:1:1:1. The temperature dependence of chemical shift for these signals indicates that 10 ^1H signals of the cyclohexane ring are distinguished and the conformation of the five-membered chelate ring is fixed at 193 K.

As shown in Figure 3, the Fe^{III} *meso*-bn chelate exhibited two peaks at 3.39 and −2.27 ppm with an area ratio of 3:1 at 303 K. These averaged signals indicate that the $\delta \rightleftarrows \lambda$ conformational interconversion of the *meso*-bn chelate is rapid on the NMR time scale. The assignment of the signals is straightforward because of the peak area ratio.

The methine and methyl signals shifted downfield accompanied by line broadening with the decrease in temperature. The former disappeared at 213 K (100 MHz), and the latter signals were observed in a near-coalescence state at 191 K (400 MHz). At 183 K, four peaks were observed with an area ratio of 0.7:3.0:2.6:0.8[45] at 51.57, 14.85, ca. 3.2, and −32.65 ppm. The peaks at both ends are due to the methine protons, and the lowest field peak was assigned to H^1 and the highest field peak to H^2 for the same reason as given for the *cis*-chxn chelate. The two signals at the center are due to the two methyl groups, one signal of which is superposed on the methanol signal. Since the (*R*)-1,2-propanediamine (*R*-pn) complex, $[Fe(CN)_4(R\text{-pn})]^-$, showed its equatorial methyl signal at 22.67 ppm at 185 K, the lower field

(45) The small intensity observed for the axial and equatorial methine protons is dependent on the reduction of an original base line that deviated severely from a straight line due to a wide range of observation frequencies (80 000 Hz).

peak was assigned to CH_3^4 and the higher field peak to CH_3^3. The chemical shift difference between H^1 and H^2 was 84.2 ppm at 183 K. This difference is larger than that observed for the *cis*-chxn chelate at 193 K. The difference between the two methyl shifts was ca. 12 ppm at 183 K. Thus the conformation of the *meso*-bn chelate is regarded to be fixed below 183 K.

For the en chelate, the averaged signal of H^1 and H^2 was observed at −1.15 ppm at 303 K, as shown in Figure 4. This signal shifted downfield with the decrease in temperature, accompanied by line broadening. Its half line width at half-height amounted to 250 Hz at 185 K, but the separate resonances corresponding to H^1 and H^2 were not observed even at 185 K. Therefore, the en chelate undergoes the most rapid interconversion among these three chelates. However, the extent of the line broadening below 213 K was large enough to estimate the rate of conformational interconversion by line-shape analysis.

Calculation of the Rate Constants of the Conformational Interconversion. The "one-way" rate constants for the $\delta \rightleftarrows \lambda$ interconversion were calculated for the ring protons by line-shape analysis from the following data: the data at 213–185 K for the en chelate; at 263–233 K for the *meso*-bn chelate; at 323–303 and 233–223 K for the *cis*-chxn chelate.

For each signal, 50 points were collected on the NMR trace at regular intervals in such a way as distributed over the range 16 times wider than the apparent half line width centered at the peak top. The line-shape analysis was performed with these points by using the Gutowsky–McCall–Slichter line-shape equation[46] (eq 1), where M_y is the total transverse magnetization, ν_{ax} and

$$M_y = \frac{E(AB + CD)}{A^2 + C^2} + F(2\pi)\nu + G \qquad (1)$$

$$A = P_{ax}/T_{2ax} + P_{eq}/T_{2eq} + P_{ax}P_{eq}(\tau_{ax} + \tau_{eq})((1/T_{2ax})(1/T_{2eq}) - \omega_{ax}\omega_{eq})$$

$$B = 1 + P_{ax}P_{eq}(\tau_{ax} + \tau_{eq})(P_{eq}/T_{2ax} + P_{ax}/T_{2eq})$$

$$C = P_{ax}\omega_{ax} + P_{eq}\omega_{eq} + P_{ax}P_{eq}(\tau_{ax} + \tau_{eq})(\omega_{eq}/T_{2ax} + \omega_{ax}/T_{2eq})$$

$$D = P_{ax}P_{eq}(\tau_{ax} + \tau_{eq})(P_{eq}\omega_{ax} + P_{eq}\omega_{eq})$$

$$\omega_{ax} = 2\pi(\nu_{ax} - \nu) \qquad \omega_{eq} = 2\pi(\nu_{eq} - \nu)$$

ν_{eq} are the intrinsic chemical shifts of the axial and equatorial ring protons (H^{ax} and H^{eq}) in the frozen conformation, T_{2ax} and T_{2eq} are the intrinsic transverse relaxation times of H^{ax} and H^{eq}, and P_{ax} and P_{eq} are the populations of the δ and λ conformers. For the present case, $P_{ax} = P_{eq} = 0.5$. E is a scaling factor required for direct comparison of the peak height, and F and G are the parameters introduced to adjust the slope and intercept of the observed base line. The τ_{ax} and τ_{eq} are the lifetimes of the δ and λ conformers, and the "one-way" rate constant, k, was obtained from the relation of $k = 2/(\tau_{ax} + \tau_{eq})$.

The fitting of the calculated line shape to the experimental one was performed by using the modified Marquardt method with simultaneous evaluation of the weight for each point by dynamic biweight method.[43] The values of chemical shifts and transverse relaxation times were fixed to the initial values. The other parameters were varied without restrictions.

The intrinsic values of the chemical shifts (ν_{ax} and ν_{eq}) and the transverse relaxation times (T_{2ax} and T_{2eq}) of each complex are expected to be strongly dependent on the temperature. Paramagnetic shifts of ^1H's arise from Fermi contact and pseudocontact shifts.[47] But the line-shape analysis for the two-sited exchange does not require the knowledge of them. Therefore the temperature dependence of ν_{ax}, ν_{eq}, T_{2ax}, and T_{2eq} were treated empirically

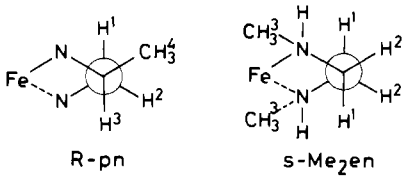

Figure 5. Schematic structures and numberings for $[Fe(CN)_4(s\text{-}Me_2en)]^-$ and $[Fe(CN)_4(R\text{-pn})]^-$ used for the reference.

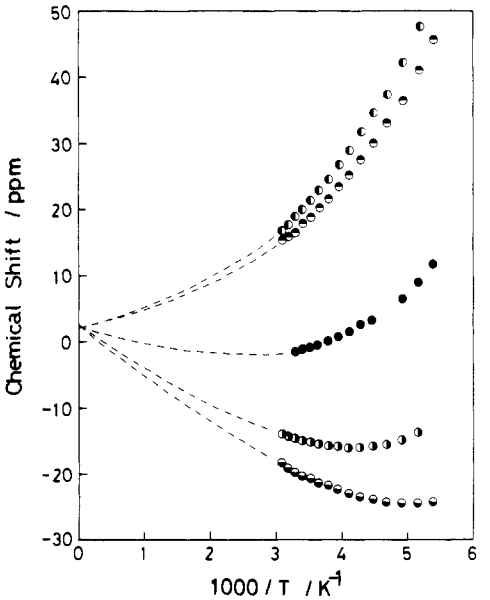

Figure 6. Temperature dependence of the chemical shift of the Fe^{III} chelates: $H^{1,3}$ (◓) and H^2 (◒) of $[Fe(CN)_4(R\text{-pn})]^-$; H^1 (◐) and H^2 (◑) of $[Fe(CN)_4(s\text{-}Me_2en)]^-$; $H^{1,2}$ (●) of $[Fe(CN)_4(en)]^-$.

by fitting polynominals to the observed values of them instead of the use of rather complicated formulations for the temperature dependency of Fermi contact shift and pseudocontact sift.[48]

Temperature Dependence of Chemical Shifts and Transverse Relaxation Times of the Ring Protons. The temperature dependence of the ^1H NMR spectra of the en, *meso*-bn, and *cis*-chxn chelates, shown in Figures 2–4, indicates that none of these low-spin paramagnetic Fe^{III} complexes obey the Curie law. In order to take the deviation from the Curie law into account, the Fe^{III} complexes, $[Fe(CN)_4(1,2\text{-diamine})]^-$ (1,2-diamine = *R*-pn, s-Me_2en), were chosen as "reference complexes", of which structures are expected to be fixed as shown in Figure 5 schematically.[39] The temperature dependence of the chemical shifts for their ring protons is shown in Figure 6.

In octahedral complexes with a five-membered chelate ring, the population of the conformer with an equatorial methyl group is estimated to be more than 90% based on the differences in $\Delta G°$ reported for several Co^{III} complexes,[2] although these complexes convert their chelate ring conformations between δ and λ. For the reference complexes in this work, the observed chemical shifts and half line widths at half-height are treated to be equal to those for their main conformers. This is justified by the large separation of H^{ax} and H^{eq} signals for them, as shown in Figure 6. The nonlinearity of the chemical shift with respect to T^{-1}, shown in Figure 6, indicates that the reference complexes also do not obey the Curie law.

For the present paramagnetic complexes, the intrinsic values of chemical shift and half line width at half-height in the frozen conformation vary with temperature. Thus the values of ν_{ax}, ν_{eq}, T_{2ax}, and T_{2eq} required for the line-shape analysis by eq 1 were estimated empirically from the corresponding values for the reference complexes.

(46) Gutowsky, H. S.; McCall, D. W.; Slichter, C. P. *J. Chem. Phys.* **1953**, *21*, 279. McConnell, H. M. *J. Chem. Phys.* **1958**, *28*, 430. The broadening of the signals by the unpaired spin is so large, as shown in Figures 2–4, that there is no necessity to take into account the splitting of the signal by scalar coupling. Therefore we used the Gutowsky–McCall–Slichter equation (1).

(47) Jesson, J. P. *The Paramagnetic Shift* in *NMR of Paramagnetic Molecules*; La Mar, G. N., Horrocks, W. D., Jr., Holm, R. H., Eds.; Academic Press: New York, 1973; pp 1–52.

(48) Theoretical treatment of the observed paramagnetic shifts will be described elsewhere with respect to the temperature dependence of Fermi contact shift and pseudocontact shift.

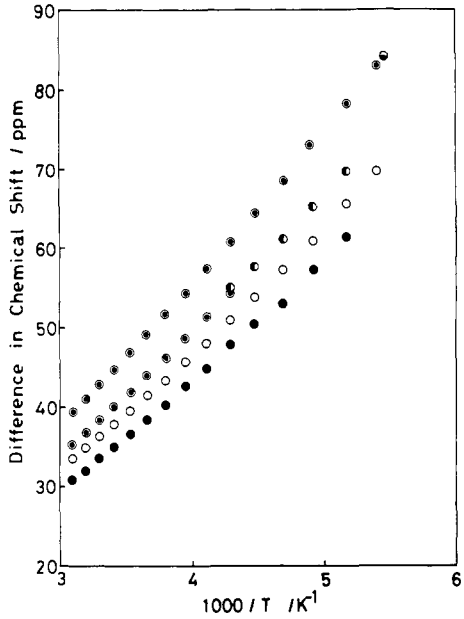

Figure 7. Temperature dependence of difference in chemical shift between axial and equatorial ring protons: (●) $[Fe(CN)_4(s\text{-}Me_2en)]^-$; (○) $[Fe(CN)_4(R\text{-pn})]^-$; (◐) $[Fe(CN)_4(cis\text{-chxn})]^-$; (⊖) $[Fe(CN)_4(meso\text{-bn})]^-$; (⊙) estimated values.

Estimation of the Intrinsic Chemical Shifts of H^{ax} and H^{eq}. The estimated differences in the intrinsic chemical shift between H^{ax} and H^{eq} in the frozen conformation, Δ, are shown in Figure 7, along with the observed Δ values for the Fe^{III} *R*-pn, s-Me_2en, *meso*-bn, and *cis*-chxn chelates.

The intrinsic Δ values were estimated as follows. An empirical equation

$$\Delta = A_1T^{-1} + A_2T^{-2} + A_3T^{-3} \quad (2)$$

was fitted to the Δ observed for the s-Me_2en chelate by varying A_1–A_3 values. The Δ values estimated with $A_1 = 6.54$, $A_2 = 1.22$, and $A_3 = -0.0391$ were in close agreement with the experimental Δ with errors of less than 1.1%. Equation 3, which is only different

$$\Delta = B(A_1T^{-1} + A_2T^{-2} + A_3T^{-3}) \quad (3)$$

from eq 2 in a scaling parameter *B*, was fitted to the Δ values observed for the *R*-pn chelate with the same values of A_1–A_3 as eq 2 with $B = 1.07$. The errors were of less than 1.4%. Thus eq 3 can be expected to hold for the present Fe^{III} complexes undergoing chelate ring interconversion.

The H^1 and H^2 signals of the *cis*-chxn chelate were observed separately at 233–193 K, as shown in Figure 2. In this temperature range, the differences between the experimental Δ and the calculated Δ from eq 3 were less than 1.3%. Keeping the parameter *B* at the value ($B = 1.14$) determined in this fitting, we evaluated the intrinsic Δ values at 323–233 K for the *cis*-chxn chelate from eq 3. The H^1 and H^2 signals of the *meso*-bn chelate were observed individually at 183 K (Figure 3). The parameter *B* was determined to be 1.28 from the experimental Δ value at 183 K. The intrinsic Δ values at 323–193 K were estimated from this *B* value. Since no separate peaks of H^1 and H^2 were observed for the en chelate even at 183 K, the intrinsic Δ for this chelate was assumed to be equal to that observed for the *R*-pn chelate. These estimated Δ values were assumed to have ±10% errors in the line-shape analysis, which are large enough to expect the true values lying within the estimated error range.

The ν_{ax} and ν_{eq} values required for the line-shape analysis were calculated from the relationships

$$\nu_{ax} = \nu_0 + C(\Delta/2) \qquad \nu_{eq} = \nu_0 - C(\Delta/2) \quad (4)$$

where ν_0 is the chemical shift for the averaged signal of H^{ax} and H^{eq}. *C* is set to unity for the central value, 1.1 for the upper limit, and 0.9 for the lower limit of the estimated ν_{ax} and ν_{eq}.

Estimation of the Intrinsic Transverse Relaxation Times of H^{ax} and H^{eq}. The intrinsic half line widths at half-height estimated for H^{ax} and H^{eq} in the frozen conformation are shown in Figure 8, as well as the experimental values for the Fe^{III} *R*-pn and s-Me_2en chelates. Since the H^{ax} and H^{eq} line-shapes observed for the reference complexes agreed closely with Lorentzian curves, the experimental values of half line widths at half-height, *W*, of H^{ax} and H^{eq} for the reference complexes were determined by fitting Lorentzian curves to the observed line shapes.

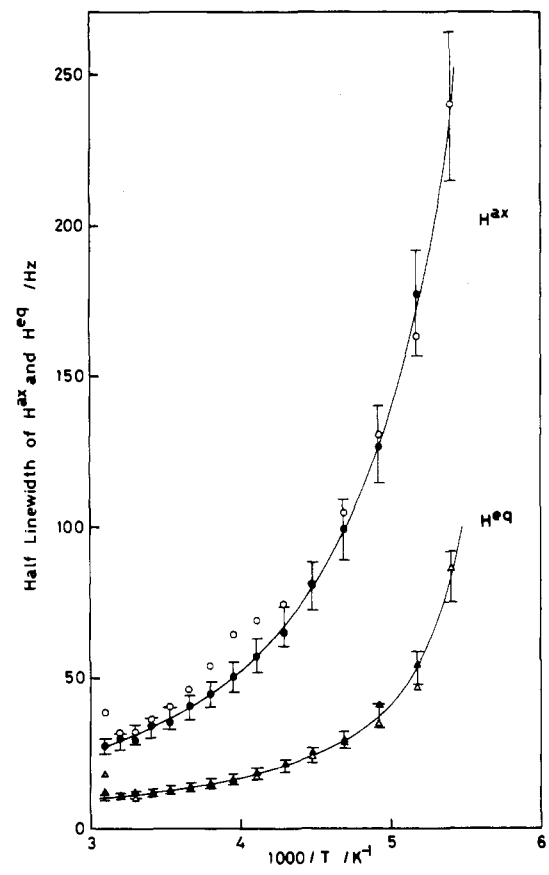

Figure 8. Temperature dependence of half line width for axial and equatorial ring protons: H^1 (●) and H^2 (▲) of $[Fe(CN)_4(s\text{-}Me_2en)]^-$; $H^{1,3}$ (○) and H^2 (△) of $[Fe(CN)_4(R\text{-pn})]^-$. The curves indicate the estimated half line widths for the axial and equatorial ring protons. The I-shaped marks indicate the maximum and minimum of the estimated half line widths.

The intrinsic *W* values were estimated for H^{ax} from the observed *W* of the s-Me_2en chelate at 323–193 K and those of the *R*-pn chelate at 203–185 K, and for H^{eq} from the observed *W* of the former at 323–193 K and those of the latter at 313–185 K. A cubic equation

$$W^{-1} = D_0 + D_1T^{-1} + D_2T^{-2} + D_3T^{-3} \quad (5)$$

was used for the estimation. The coefficients D_0–D_3 were obtained as $D_0 = 28.3$, $D_1 = -597$, $D_2 = 3320$, and $D_3 = -4310$ for the H^{ax} peak and as $D_0 = -243$, $D_1 = 2010$, $D_2 = -4040$, and $D_3 = 3350$ for the H^{eq} peak from the fitting of eq 5 to the *W* values observed for H^{ax} and H^{eq} of the reference complexes. Fixing these coefficients allowed the intrinsic *W* values at each temperature to be estimated by eq 5. A sufficiently large error of ±10% was assumed for each estimated *W* value so that the corresponding true value should lie within the limits of error. The line broadening due to the increase in viscosity of the solution on cooling was canceled out by estimation of the intrinsic *W* values for the en, *meso*-bn, and *cis*-chxn chelates from those for the reference complexes obtained under the same conditions.

The transverse relaxation time, T_2, required for eq 1 were obtained from the relationship of $T_2 = (2\pi W)^{-1}$.

Calculation of the Activation Parameters. The activation parameters were calculated from the Eyring equation[49]

$$k = \kappa(k_BT/h)[\exp(-\Delta H^*/RT)][\exp(\Delta S^*/R)] \quad (6)$$

Table I. Activation Parameters for the $\delta \rightleftarrows \lambda$ Conformational Interconversion of $[Fe(CN)_4(1,2\text{-diamine})]^-$ in CD_3OD-DCl

diamine	$\Delta H^{\ddagger}$/kJ mol^{-1}	$\Delta S^{\ddagger}$/J K^{-1} mol^{-1}	$\Delta G^{\ddagger}_{298}$/kJ mol^{-1}
en	24.7 ± 4.5	0.0 ± 27.0	24.7 ± 3.6
meso-bn	30.1 ± 3.9	−2.9 ± 19.1	31.0 ± 1.8
cis-chxn	42.7 ± 2.0	−7.7 ± 8.4	45.0 ± 0.5

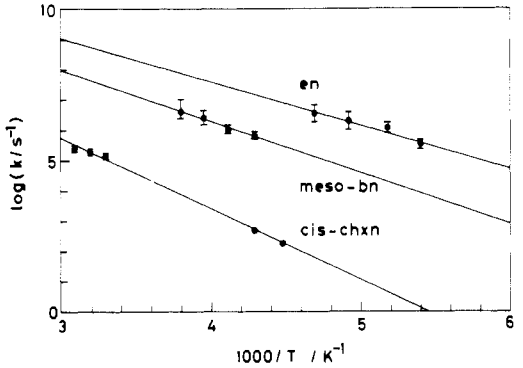

Figure 9. Arrhenius plots for the $\delta \rightleftarrows \lambda$ conformational interconversion of the chelate ring of $[Fe(CN)_4(1,2\text{-diamine})]^-$ in CD_3OD-DCl.

where k_B is the Boltzmann constant and κ a transmission coefficient, which was set to unity. The $\Delta H^{\ddagger}$ and $\Delta S^{\ddagger}$ values were obtained by a weighted least-squares linear regression analysis of $-R[\ln (kh/k_BT)]$ on T^{-1} and are summarized in Table I. The Arrhenius plots for the en, *meso*-bn, and *cis*-chxn chelates are shown in Figure 9.

The errors in the activation parameters are primarily derived from the estimated values of the intrinsic chemical shifts and the intrinsic transverse relaxation times for H^{ax} and H^{eq}. Errors in temperature (±1 K) and chemical shifts determined experimentally were much smaller than the estimation errors.

Discussion

Application of Paramagnetic Shift to Line-Shape Analysis. The rate constant, k, for the conformational interconversion of the chelate ring can be obtained by NMR line-shape analysis, when $\delta W < k < \Delta^2/\delta W$,[50] where δW is the increase in half line width at half-height due to the interconversion. Since usual diamagnetic compounds have Δ of 0.5–3 ppm and δW of a few hertz, the magnitude of k measured with a 100-MHz ^{1}H NMR spectrometer is at most on the order of 10^4 s^{-1}.

For the paramagnetic Fe^{III} complexes used in this work, the observed Δ was greater than 30 ppm and the mean half line width of H^{ax} and H^{eq} was larger than 20 Hz. Moreover, the chelates shown in Figure 1 are appropriate to the determination of the conformational interconversion rate, because the largest line broadening by the interconversion is expected for the system in which the δ and λ forms are identical in energy and the population is 1:1. Therefore, the limit of k is expected to go up to 10^6 s^{-1}, if k can be determined when δW is greater than 10 Hz. This prediction has been verified as shown in Figure 9. The k values of $>10^7$ s^{-1} can be determined from the analogous measurement under much higher magnetic fields.

Rates and Activation Parameters for the $\delta \rightleftarrows \lambda$ Interconversion. Five-membered chelate rings are formed by the coordination of bidentate ligands to metal ions, such as 1,2-diamines, amino alcohols, amino acids, diarsines, thioethers, and selenoethers.[2] However, the rates and activation parameters for the $\delta \rightleftarrows \lambda$ interconversion of the chelate ring have been reported for the *N,N,N',N'*-tetramethylethanediamine (tmen) complexes such as $[Co^{III}(NO)_2(tmen)]^+$,[31] $[Zn^{II}Cl_2(tmen)]$,[31] $[M^0(CO)_4(tmen)]$ (M = Cr, Mo, and W),[33] and $[Pr^{III}([^2H_9]fod)_3(tmen)]$[32] and La^{III} 1,4,7,10-tetraazacyclododecane-*N,N',N'',N'''*-tetraacetate.[34] The k values obtained from these studies are on the order of 10^6 s^{-1} at 300 K.

The activation parameters obtained for the Fe^{III} complexes, $[Fe(CN)_4(1,2\text{-diamine})]^-$ (1,2-diamine = en, *meso*-bn, and *cis*-chxn) are summerized in Table I. The interconversion rates for these chelates at 298 K are ca. 3×10^8, 2×10^7, and 8×10^4 s^{-1} respectively. The order of magnitude for the $\Delta H^{\ddagger}$ and $\Delta G^{\ddagger}$ is *cis*-chxn > *meso*-bn > en. The $\Delta S^{\ddagger}$ values are close to zero and have a tendency to become negative with an increase in the bulkiness of the substituent group.

The $\Delta H^{\ddagger}$ for the en chelate is 24.7 kJ mol^{-1}. Gollogly et al. have reported the results of strain-energy minimization calculation for the $\delta \rightleftarrows \lambda$ interconversion of tris(ethanediamine)cobalt complexes with the metal–nitrogen distance of 200 pm.[51] The transition state has an envelope structure with a barrier of 20 kJ mol^{-1}. This $\Delta H^{\ddagger}$ value is almost equal to the present experimental value within the estimation error. This agreement supports the mechanism that the $\delta \rightleftarrows \lambda$ interconversion proceeds through an envelope conformation. From the activation parameters obtained in this work, the separate resonances for H^1 and H^2 of the en chelate are presumed to be observed below 150 K.

The *meso*-bn chelate is regarded as a methyl-substituted derivative of the en chelate, so that if the *meso*-bn takes the envelope form in the transition state of the $\delta \rightleftarrows \lambda$ interconversion, the $\Delta H^{\ddagger}$ for the *meso*-bn chelate will be higher than that for the en chelate by the repulsion energy between the two methyl groups. This increment in $\Delta H^{\ddagger}$ is estimated to be 3.1 kJ mol^{-1} from the difference in rotation energy barrier between ethane (12.1 kJ mol^{-1})[52] and *n*-butane (15.2 kJ mol^{-1}).[53] Thus the estimate of the $\Delta H^{\ddagger}$ for the *meso*-bn chelate is 27.8 kJ mol^{-1} and is in agreement with the observed value, 30.1 kJ mol^{-1}, within the estimation error. Therefore the $\delta \rightleftarrows \lambda$ interconversion for the *meso*-bn chelate is expected to proceed through the envelope form as well as the en chelate.

The difference in $\Delta H^{\ddagger}$ between the *meso*-bn and en chelates, 5.4 kJ mol^{-1}, is regarded as the repulsion energy between the two methyl groups in the envelope form. The difference in $\Delta H^{\ddagger}$ between the present Fe^{III} en chelate and the Cr^0 tmen complex (39.4 kJ mol^{-1})[33] is 14.7 kJ mol^{-1}. As the metal–nitrogen bond length is almost the same between them, this difference is attributable to the four *N*-methyl groups of tmen. Therefore, the repulsion energy due to a *N*-methyl group is estimated as ca. 3.7 kJ mol^{-1}.

The *cis*-chxn chelate has a five-membered chelate ring condensed with a cyclohexane ring, so that the $\delta \rightleftarrows \lambda$ interconversion is inevitably accompanied by the conformational change of the cyclohexane ring. Cyclohexane is known to convert the conformation as follows: chair → half-chair → skew-boat → boat → skew-boat → half-chair → chair.[54] The half-chair, twist-boat, and boat forms have been estimated to be 45.6, 23.8, and 26.8 kJ mol^{-1} higher in energy than the chair form, respectively.[55] If the transition state for the *cis*-chxn chelate is the envelope form, the cyclohexane ring is in a boat conformation. The energy for this structure is expected to be equal to 39.5 kJ mol^{-1}, which is obtained from $\Delta H^{\ddagger}_1$ for the en chelate, the energy difference, ΔH°_2, between chair and boat forms of cyclohexane, and the repulsion energy, ΔH_3, between the eclipsed hydrogen atoms as follows: $(\Delta H^{\ddagger}_1 - \Delta H_3) + (\Delta H^{\circ}_2 - 2\Delta H_3) = 39.5$ kJ mol^{-1}. This is in agreement with the $\Delta H^{\ddagger}$ value obtained in this work. Therefore the envelope structure is expected as the transition state for the *cis*-chxn chelate as well as the en and *meso*-bn chelates, and the increase in $\Delta H^{\ddagger}$ compared to that of en chelate can be explained by the larger steric repulsion energy due to the cyclohexane ring.

(49) Eyring, H. *J. Chem. Phys.* **1935**, *3*, 107.
(50) Carrington, A.; McLachlan, A. D. *Introduction to Magnetic Resonance with Applications to Chemistry and Chemical Physics*; Harper and Row: New York, 1967; Chapter 12.
(51) Gollogly, J. R.; Hawkins, C. J.; Beattie, J. K. *Inorg. Chem.* **1971**, *10*, 317.
(52) Hirota, E.; Saito, S.; Endo, Y. *J. Chem. Phys.* **1979**, *71*, 1183.
(53) Compton, D. A. C.; Montero, S.; Murphy, W. F. *J. Phys. Chem.* **1980**, *84*, 3587.
(54) Morison, R. T.; Boyd, R. N. *Organic Chemistry*; Allyn and Bacon: Boston, MA, London, Sydney, Australia, Toronto, Canada, 1983; p 178.
(55) Wiberg, K. B.; Boyd, R. H. *J. Am. Chem. Soc.* **1972**, *94*, 8426.

Another plausible transition state is a gauche form of the chelate ring with a cyclohexane ring in a half-chair conformation. The $\Delta H^{\ddagger}$ values for *cis*-1,2-, *trans*-1,3-, and *cis*-1,4-dimethylcyclohexane have been reported to be 42.30, 43.85, and 44.10 kJ mol^{-1} respectively.[56] These values are close to those for cyclohexane: 43.1-48.1 kJ mol^{-1}.[57-59] Eclipsing of vicinal methyl groups, which must take place at some stage in the conformational change of cyclohexane, can occur during pseudorotation of the twist-boat form via the boat form, which is about 19 kJ mol^{-1} lower[55] in energy than the half-chair form, in a manner similar to that for 1,2- and 1,2,4,5-substituted cyclohexanes reported by Wolfe and Campbell.[60] An organic counterpart of the *cis*-chxn chelate is *cis*-bicyclo[4,3,0]nonane (*cis*-bcn), and its $\Delta H^{\ddagger}$ for the conformational change has been reported to be 37.0 kJ mol^{-1}.[61] The molecular force field calculation has shown that the cyclohexane ring takes a half-chair form at the transition stage, where the dihedral angle of the C^9-C^1-C^2-C^3 moiety is 125°.[61] The decrease in $\Delta H^{\ddagger}$ observed for *cis*-bcn compared with cyclohexane is attributable to the strain energy of the cyclopentane ring, which is estimated as 5.4 kJ mol^{-1} on the basis of the strain energies of *cis*-bcn (41.1 kJ mol^{-1}),[62] cyclohexane (5.65 kJ mol^{-1}),[62] and cyclopentane (30.1 kJ mol^{-1}),[62] assuming that the strain energy of the cyclopentane ring is maintained constant during the conformational change. Since the $\Delta H^{\ddagger}$ observed for the *cis*-chxn chelate is similar in magnitude to the values for cyclohexane and dimethylcyclohexanes, the half-chair form of the cyclohexane ring is another plausible transition state.

We have reported here some basic data with respect to the conformational interconversion between δ and λ forms of five-membered chelate ring. Since the $\Delta G^{\ddagger}$ values so far reported for the $\delta \rightleftarrows \lambda$ interconversion[33] are almost independent of the variation of the central metal ion, the results in this work are expected to be valid for other metal chelates. This study also demonstrated that the application of paramagnetic shift to NMR line-shape analysis is useful for fast dynamic process, e.g., the conformational interconversion.

Acknowledgment. The present study was supported by a Grant-in-Aid for Scientific Research (No. 61540452) from the Ministry of Education, Science and Culture, Japan. We thank Setsuko Kato for obtaining the 400-MHz ^{1}H NMR data.

(56) Mann, B. E. *J. Chem. Soc., Perkin Trans. 2* **1977**, 84.
(57) Anet, F. A. L.; Bourne, A. J. R. *J. Am. Chem. Soc.* **1967**, *89*, 760.
(58) Höfner, D.; Lesko, S. A.; Binsch, G. *Org. Magn. Reson.* **1978**, *11*, 179.
(59) Poupko, R.; Luz, Z. *J. Chem. Phys.* **1981**, *75*, 1675.
(60) Wolfe, S.; Campbell, J. R. *Chem. Commun.* **1967**, 874.
(61) Schneider, H.-J.; Nguyen-Ba, N. *Org. Magn. Reson.* **1982**, *18*, 38.
(62) Schleyer, P. v. R.; Williams, J. E., Jr.; Blanchard, K. R. *J. Am. Chem. Soc.* **1970**, *92*, 2377.

Contribution from the University Chemical Laboratory, Lensfield Road, Cambridge CB2 1EW, England

Energetics of Metal Complex Isomerization Reactions

Brian F. G. Johnson* and Alison Rodger*,†

Received May 18, 1988

A stereochemical approach to transition-metal complex geometry is coupled to a recently developed model for the energetics of such systems to enable rearrangement mechanisms to be compared and the most favorable one to be determined. A useful notation for discussing such reactions is also developed.

A recently developed model, which enables a semiquantitative determination of the most stable geometry of an ML_n system,[1] can equally well be applied to proposed transition states in rearrangement processes to determine the one of lowest energy. In conjunction with a classical symmetry selection rule procedure (CSRP)[2,3] for determining reaction mechanisms, we should be able to understand why some transition-metal complexes are fluxional (i.e. isomerize on an NMR time scale), others rearrange on longer time scales (isomerization), and others are effectively stable. In addition, it should be possible to determine the relative probabilities of proposed mechanisms. It has already been possible[4] to determine the conditions under which the Ray-Dutt tris chelate metal complex isomerization mechanism is favored over the Bailar twist mechanism.

The model for the energetics of coordination compounds of the type ML_n resulted from considering the following expression for the energy of the molecule

$$E(ML_n) = \sum M\text{-}L + \sum L\text{-}L + \sum el \qquad (1)$$

where $\sum$M-L includes all the M-L bonding energy, $\sum$L-L includes the ligand-ligand interactions and $\sum$el includes the energetic contribution made by the nonbonding electron density. For our current purposes, we shall simply report the conclusions appropriate for the systems we are studying and illustrate them by application. Further details can be found in ref 1. (i) In general if the M-L bond length remains constant at its "optimal length" then $\sum$M-L is approximately independent of the orientation of the ligands, L. (ii) $\sum$el (or its change as a function of different L orientations) is not the dominant contribution to the energy for bond angles greater than 90°. (The conclusions of our study contrast with the valence-shell electron-pair repulsion model of molecular geometry which assumes that a very significant stabilizing factor is the formation of localized electron pairs from any nonbonding valence electrons.) (iii) $\sum$L-L can be expressed as the sum of a short-range L-L repulsive potential energy (most conveniently approximated by a hard-sphere potential), plus an L-L attractive r^{-6} dispersion energy (where r is the L-L distance), plus (if appropriate) a r^{-1} charge-charge interaction energy (which is usually repulsive). In the present work, we shall exclude from our explicit consideration systems where charge-charge interactions are significant (in conjunction with ref 1 the extension to include such systems is straightforward). Thus, we shall consider systems where the ligand orientation is such that it maximizes the dispersive ligand attraction subject to hard-sphere radii that define the smallest L-L distance. Further details of how to estimate dispersion energies are given in ref 1. Two points should be noted about this approach to energetics. First, it was developed by considering all the interactions within a molecule and is not merely an empirical fit to a postulated form. Second, the *attractive* dispersion energies proved to play a large role in the determination

† Present address: Physical Chemistry Laboratory, South Parks Road, Oxford OX1 3QZ, England.

(1) Rodger, A.; Johnson, B. F. G. *Inorg. Chim. Acta* **1988**, *146*, 35.
(2) Rodger, A.; Schipper, P. E. *Inorg. Chem.* **1988**, *27*, 458.
(3) Schipper, P. E.; Rodger, A. In preparation.
(4) Rodger, A.; Johnson, B. F. G. *Inorg. Chem.* **1988**, *27*, 3061.

0020-1669/89/1328-1003$01.50/0